9th U.S. National Combustion Meeting
Organized by the Central States Section of the Combustion Institute
May 17–20, 2015
Cincinnati, Ohio

A Numerical and Experimental Study of Coflow Laminar Diffusion Flames: Effects of Gravity and Inlet Velocity

S. Cao[1] *B.A.V. Bennett*[1] *B. Ma*[2] *D. Giassi*[1] *D.P. Stocker*[3]
F. Takahashi[4] *M.B. Long*[1] *M.D. Smooke*[1,*]

[1]*Department of Mechanical Engineering & Materials Science, Yale University, P.O. Box 208284, New Haven, Connecticut 06520–8284 USA*

[2]*GE Global Research Center, 1 Research Circle, Niskayuna, NY 12309, USA*

[3]*NASA Glenn Research Center, Cleveland, Ohio 44135 USA*

[4] *Department of Mechanical & Aerospace Engineering, Case Western Reserve University, Cleveland, Ohio 44106 USA*

[*]*Corresponding Author Email: mitchell.smooke@yale.edu*

Abstract: In this work, the influence of gravity, fuel dilution, and inlet velocity on the structure, stabilization, and sooting behavior of laminar coflow methane-air diffusion flames was investigated both computationally and experimentally. A series of flames measured in the Structure and Liftoff in Combustion Experiment (SLICE) was assessed numerically under microgravity and normal gravity conditions with the fuel stream CH_4 mole fraction ranging from 0.4 to 1.0. Computationally, the MC-Smooth vorticity-velocity formulation of the governing equations was employed to describe the reactive gaseous mixture; the soot evolution process was considered as a classical aerosol dynamics problem and was represented by the sectional aerosol equations. Since each flame is axisymmetric, a two-dimensional computational domain was employed, where the grid on the axisymmetric domain was a nonuniform tensor product mesh. The governing equations and boundary conditions were discretized on the mesh by a nine-point finite difference stencil, with the convective terms approximated by a monotonic upwind scheme and all other derivatives approximated by centered differences. The resulting set of fully coupled, strongly nonlinear equations was solved simultaneously using a damped, modified Newton's method and a nested Bi-CGSTAB linear algebra solver. Experimentally, the flame shape, size, lift-off height, and soot temperature were determined by flame emission images recorded by a digital camera, and the soot volume fraction was quantified through an absolute light calibration using a thermocouple. For a broad spectrum of flames in microgravity and normal gravity, the computed and measured flame quantities (e.g., temperature profile, flame shape, lift-off height, and soot volume fraction) were first compared to assess the accuracy of the numerical model. After its validity was established, the influence of gravity, fuel dilution, and inlet velocity on the structure, stabilization, and sooting tendency of laminar coflow methane-air diffusion flames was explored further by examining quantities derived from the computational results.

Keywords: laminar diffusion flame, gravity, fuel dilution, flame structure

1 Introduction

In 2011, over 70% of electricity in U.S. was generated from the burning of fossil fuels, so a better understanding of combustion is of great importance [1]. Microgravity provides an ideal yet rigorous environment to study flame structure and examine computational models, because the structure of a microgravity flame is dramatically different from its normal gravity counterpart, and microgravity flames have larger scales and longer residence times, which makes it possible to study a wider range of flame conditions than under normal gravity. As a result, a significant amount of research has been conducted under microgravity conditions (e.g., [2–7]) to study the effects of various physical parameters on flames. In this study, previous computational and experimental investigations of coflow laminar diffusion flames (e.g., [2, 3, 8, 9]) were extended to explore further the influences of gravity, fuel dilution, and inlet velocity on the structure and stabilization of laminar coflow methane/air diffusion flames.

2 Burner configuration

The burner consists of a central jet, from which the fuel mixture issues, and a surrounding coaxial square duct, from which the coflow air flows. The inner jet's inner radius is $r_{\mathrm{I}} = 0.162$ cm and its wall thickness is $w_{\mathrm{JET}} = 0.028$ cm. The square duct's width is 7.62 cm. Details of the burner construction and operation are provided in [8]. Thirty 70% $\mathrm{CH_4}$ flames have been studied at three inlet fuel velocities ($v_{\mathrm{F}} = 23$ cm/s, 46 cm/s, and 81 cm/s) and five coflow velocities (peak coflow velocity $v_{\mathrm{O,max}}$ approximately equals to 18, 39, 48, 54, and 71 cm/s) under both microgravity ($\mu\mathrm{g}$) and normal gravity ($1\,\mathrm{g}$). Since each flame is surrounded by an air coflow and takes at most 4% of the cross-sectional area of the burner, the square duct is approximated as a coaxial tube with an identical cross-sectional area (radius $r_{\mathrm{O}} = 4.288$ cm); see Fig. 1 (left). The velocity profile of the fuel stream is parabolic, with the average Reynolds number in the fuel jet ranging from 21 to 76. Due to hardware imperfections, the flow field of the coflow air is not perfectly flat and has a bump near the inner tube; see Fig. 1 (right). To capture this nonideality, the measured inlet velocity distribution has been fitted by a hyperbolic tangent function [8, 9]. Since temperature measurements near the fuel tube exit are unavailable, the inlet temperature is set to 298 K.

3 Computational approach

The numerical framework is similar to those in the authors' previous works (see, for example, [10–13]) with the MC-Smooth vorticity-velocity formulation [14] employed. Specifically, the gaseous mixture is assumed to be Newtonian, and the diffusion of each species is approximated as Fickian. The flow's small Mach number implies that pressure P can be approximated as being independent of location in the flame, and mixture density ρ can be directly obtained from the ideal gas law. To evaluate the divergence of the net radiative flux, the model includes an optically thin radiation submodel [15–17] with three radiating species ($\mathrm{H_2O}$, CO, and $\mathrm{CO_2}$). The gas-phase chemistry employed in this research is the GRI 3.0 mechanism [18] with all nitrogen-containing species (except $\mathrm{N_2}$) removed, leaving 35 species and 217 reactions. All thermodynamic, chemical, and transport properties are evaluated by the CHEMKIN [19, 20] and TRANSPORT [21, 22] subroutine libraries, parts of which were optimized for greater speed [23].

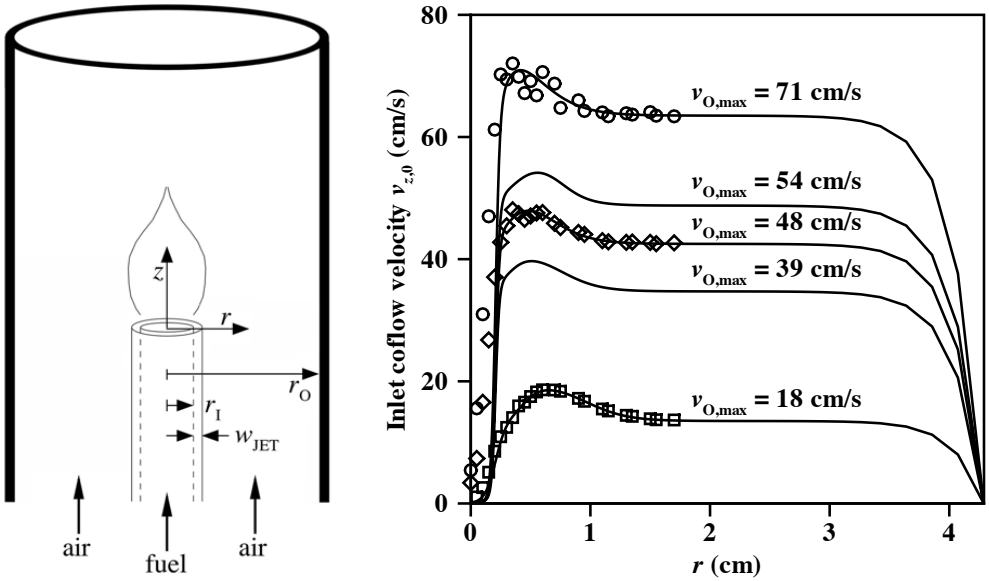

Figure 1: Left: Schematic of the burner used in the simulations. Right: Measured (symbols) and fitted (line) velocity profiles of the coflow air.

Since each flame is axisymmetric, a two-dimensional computational domain is employed, extending radially to $r = 4.288$ cm and axially to $z = 12.2$ cm. Except for the specific values of velocities, temperatures, and concentrations at the inlet, the boundary conditions are similar to those in [11, 24] and are outlined here briefly. At the bottom boundary (inlet), v_r, v_z, T, and Y_n $(n = 1, ..., N_{\text{species}})$ are specified to values mentioned previously in Section 2, and the definition of ω is applied. At the top boundary (outlet), the definition of ω is applied, and axial gradients of all other variables vanish. Along the axis of symmetry (z-axis), v_r and ω vanish; $\partial v_z/\partial r$, $\partial T/\partial r$, and $\partial Y_n/\partial r$ $(n = 1, ..., N_{\text{species}})$ are set to zero. The boundary conditions on v_z, T, and Y_n are discretized as discussed in [11], in order to avoid convergence difficulties and/or discretization inaccuracies. At the outer radial boundary, v_r, v_z, and $\partial Y_n/\partial r$ $(n = 1, ..., N_{\text{species}})$ vanish, $T = 298$ K, and the definition of ω is applied.

The grid on the axisymmetric domain is a nonuniform tensor product mesh containing 129 points in the r direction and 202 points in the z direction. The grid points are clustered towards the burner surface and the centerline in order to capture the sharp gradients in these regions. The governing equations and boundary conditions were then discretized on this tensor product grid via standard nine-point finite difference stencils, which are second-order accurate in the regions of the grid that are equispaced and are between first- and second-order accurate elsewhere. The resulting set of fully coupled, highly nonlinear equations is then solved simultaneously at all grid points using a damped modified Newton's method [25, 26] with a nested Bi-CGSTAB linear algebra solver [27]. To aid in convergence of Newton's method, pseudo-transient continuation is performed until the adaptively chosen pseudo-time step exceeds a cut-off value, after which the steady-state equations are finally solved to a Newton tolerance of 10^{-4}. All calculations were performed on workstations with 3.0-GHz Intel Xeon E5472 processors, and the typical memory usage for a computation on the 129×202 grid is around 2.2 GB of RAM.

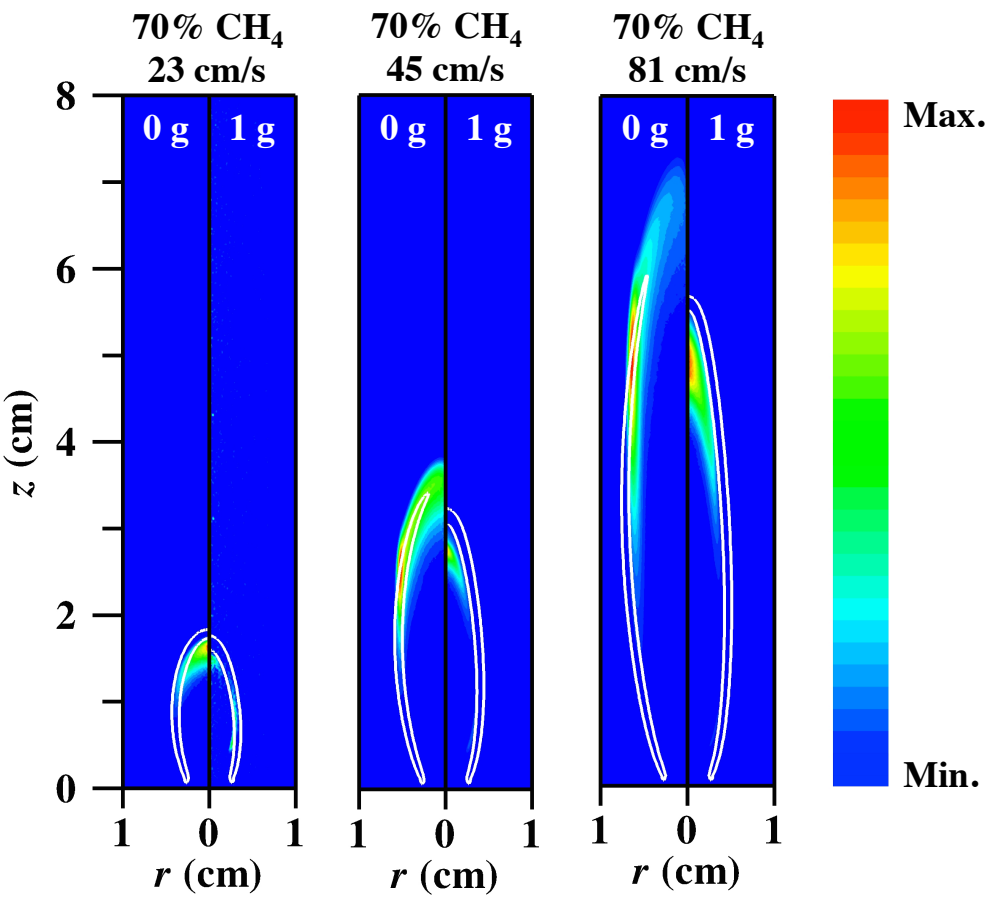

Figure 2: Typical results of computed and measured luminous flame shapes illustrating effects of inlet fuel velocity. Color contours are measured luminous flame images, and white isopleths are computed luminous flame boundaries defined by contours of 1% of the maximum CH concentration. Flame parameters are shown at the top of each plot.

4 Experimental approach

A digital single lens reflex camera was used for flame shape measurement and was fully characterized as a ratio pyrometer for soot temperature measurement. The spectral responses of the red, green, and blue channels have been measured following the approach detailed in [28, 29]. A calculated lookup table that correlates color ratio and soot temperature is used to determine the axisymmetric soot temperature distribution. Further details can be found in [8].

5 Preliminary results and discussion

The numerical model has been validated for buoyant and nonbuoyant coflow laminar diffusion flames in previous research [8, 9]. In this work, additional validation was conducted by comparing the computed and measured luminous flame shapes of a series of CH_4-air coflow laminar diffusion flames in both μ g and 1 g. Figure 2 shows a comparison between computed and measured luminous flame shapes at identical fuel dilution level to demonstrate the effects of inlet velocity and gravity on flame geometry. This direct comparison was enabled by the previous observation [2]

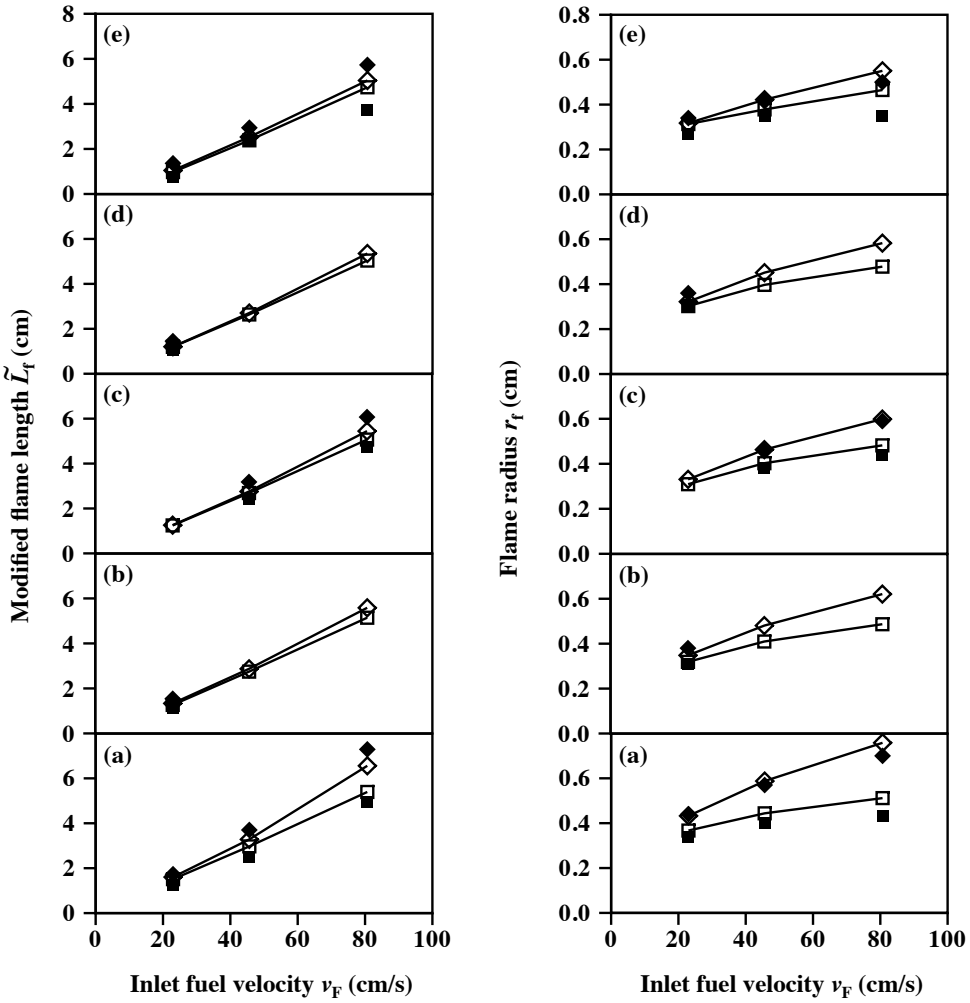

Figure 3: Left: Effect of inlet fuel velocity and inlet coflow velocity on modified flame length. Right: Effect of inlet fuel velocity and inlet coflow velocity on flame radii. In both plots, closed symbols denote measurements, and solid lines with open symbols denote predictions; squares denote results at 1 g, and diamonds denote results at μ g. Plots (a), (b), (c), (d), and (e) correspond to data with peak coflow velocity set to 18, 39, 48, 54, and 71 cm/s.

that excellent structural agreement exists between computed CH and measured CH^* in CH_4-air diffusion flames for flame shape and lift-off height in both μ g and 1 g. Since the flames studied in our work range from lifted, non-sooting flames to attached, sooting flames, we defined the computed luminous flame boundary as the contour of 1% of the maximum CH concentration to ensure data consistency. Regardless of the presence of soot, there is generally good agreement between computed and measured flame shapes: the computed luminous flame boundaries are located very close to the measured ones, and they capture the tendency that the flames become longer and wider as buoyancy is eliminated or fuel concentration is increased.

Figure 3 shows the effects of inlet fuel velocity, inlet coflow velocity, and gravity on the modified flame length (obtained by subtracting the lift-off height from the flame length) and flame radius of coflow laminar methane-air diffusion flames. From Fig. 3, we can see that in most flames, the agreement between computations and experiments is very good. In addition, we can also find that

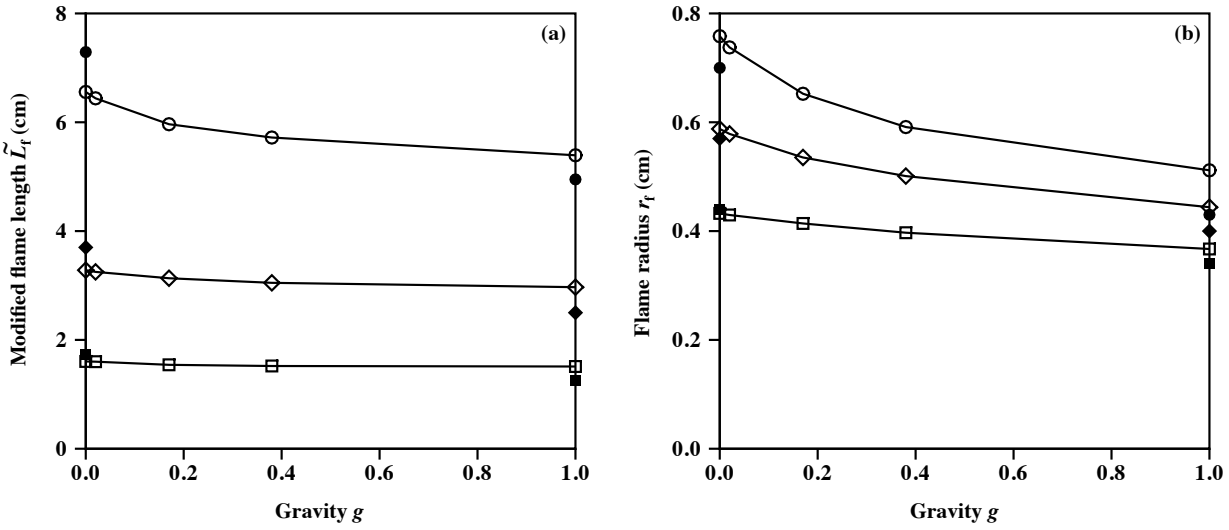

Figure 4: Effects of gravitational acceleration on (a) modified flame length and (b) flame radius of 70% CH_4 flames. In both plots, closed symbols denote measurements, solid lines with open symbols denote predictions. Results with inlet fuel velocities equal to 23 cm/s, 45 cm/s, and 81 cm/s are denoted by squares, diamonds, and circles.

for a fixed coflow velocity, increasing the fuel velocity will effectively increase the length and the radius of the flame. On the other hand, increasing the coflow velocity will reduce both the modified flame length and the flame radius. Furthermore, it can be seen from Fig. 3 that changing gravity also has a significant impact on laminar diffusion flames. Specifically, when gravitational acceleration is eliminated, the flame becomes longer and wider, and the actual difference (i.e., on an absolute basis) between μ g flame and 1 g flame will increase when the inlet fuel velocity is increased or the inlet coflow velocity is reduced.

Finally, we will take a closer look at the effects of gravity on flame structure. In Fig. 4, we have employed a total of five gravitational acceleration levels, 0 g, 0.02 g (typical value of the g-jitter on aircraft flying parabolic trajectories), 0.17 g (gravitational acceleration on Moon), 0.38 g (gravitational acceleration on Mars), and 1.0 g (gravitational acceleration on earth). From the results in Fig. 4, we see that the effects of gravity on flame structure are highly nonlinear, and the flame shape changes much faster near 0 g than near 1 g. In addition, we also see that this nonlinearity increases with increasing inlet fuel velocity, and this effect is particularly obvious in the flame radii results. This result is not surprising because the buoyant acceleration is countered by buoyant entrainment such that gravity tends to have a limited effect on the flame height. In contrast, buoyant entrainment tends to narrow these flames.

Further numerical investigations are in progress. In particular, the effect of fuel stream dilution (e.g., 40% CH_4 and 100% CH_4) will be explored at a series of coflow velocities by comparison with corresponding experimental measurements. After that, the sooting behavior of these flames will also be examined.

6 Acknowledgments

The authors would like to acknowledge support for this work from the U.S. Department of Energy Office of Basic Energy Sciences under Award Number DE-FG02-88ER13966 (Dr. Mark Pederson, contract monitor); the National Science Foundation CBET-0828802 (Dr. Phil Westmoreland, contract monitor); NASA NNX11AP43A (Mr. Dennis P. Stocker, contract monitor); the U.S. Air Force Office of Scientific Research AFOSR FA9550-12-1-0157 (Dr. Chiping Li and Dr. Fariba Fahroo, contract monitors); and the Strategic Environmental Research and Development Program and the Air Force Research Laboratory under agreement number FA8650-10-2-2934.

References

[1] U.S. Energy Information Administration (2011). Electricity Explained — Basics.

[2] K.T. Walsh, J. Fielding, M.D. Smooke, M.B. Long, A. Liñán, Proc. Combust. Inst. 30 (2005) 357–365.

[3] K.T. Walsh, J. Fielding, M.D. Smooke, M.B. Long, Proc. Combust. Inst. 28 (2000) 1973–1979.

[4] M.R.J. Charest, C.P.T. Groth, Ö.L. Gülder, Combust. Flame 158 (10) (2011) 1933–1945.

[5] I. Glassman, Proc. Combust. Inst. 27 (1998) 1589–1596.

[6] M.R.J. Charest, C.P.T. Groth, Ö.L. Gülder, Combust. Flame 158 (5) (2011) 860–875.

[7] S.K. Aggarwal, Prog. Energy Combust. Sci. 35 (6) (2009) 528–570.

[8] B. Ma, S. Cao, D. Giassi, D.P. Stocker, F. Takahashi, B.A.V. Bennett, M.D. Smooke, M.B. Long, Proc. Combust. Inst. 35 (2015) 839–846.

[9] S. Cao, B. Ma, B.A.V. Bennett, D. Giassi, D.P. Stocker, F. Takahashi, M.B. Long, M.D. Smooke, Proc. Combust. Inst. 35 (2015) 897–903.

[10] B.A.V. Bennett, C.S. McEnally, L.D. Pfefferle, M.D. Smooke, Combust. Flame, 123 (4) (2000) 522–546.

[11] B.A.V. Bennett, M.D. Smooke, Combust. Theory Model. 2 (1998) 221–258.

[12] M.D. Smooke, R.J. Hall, M.B. Colket, J. Fielding, M.B. Long, C.S. McEnally, L.D. Pfefferle, Combust. Theory Model. 8 (3) (2004) 593–606.

[13] M.D. Smooke, M.B. Long, B.C. Connelly, M.B. Colket, R.J. Hall, Combust. Flame 143 (4) (2005) 613–628.

[14] S. Cao, B.A.V. Bennett, M.D. Smooke, Combust. Theory Model. submitted.

[15] D.K. Edwards, Adv. Heat Transfer 12 (1976) 115–193.

[16] R.J. Hall, J. Quant. Spectrosc. Radiat. Transfer 49 (5) (1993) 517–523.

[17] R.J. Hall, J. Quant. Spectrosc. Radiat. Transfer 51 (4) (1994) 635–644.

[18] G.P. Smith, D.M. Golden, M. Frenklach, N.W. Moriarty, B. Eiteneer, M. Golderberg, C.T. Bowman, R.K. Hanson, S. Song, W.C. Gardiner, Jr., V.V. Lissianski, Z. Qin, GRI-Mech 3.0, 1999; available at <http://www.me.berkeley.edu/gri_mech>.

[19] R.J. Kee, J.A. Miller, T.H. Jefferson, Chemkin: A general-purpose, problem-independent, transportable, Fortran chemical kinetics code package, Report No. SAND80-8003, Sandia National Laboratories, 1980.

[20] R.J. Kee, F.M. Rupley, J.A. Miller, The Chemkin thermodynamic database, Report No. SAND87-8215, Sandia National Laboratories, 1987.

[21] R.J. Kee, J. Warnatz, J.A. Miller, A Fortran computer code package for the evaluation of gas-phase viscosities, conductivities, and diffusion coefficients, Report No. SAND83-8209, Sandia National Laboratories, 1983.

[22] R.J. Kee, G. Dixon-Lewis, J. Warnatz, M.E. Coltrin, J.A. Miller, A Fortran computer package for the evaluation of gas-phase, multicomponent transport properties, Report No. SAND86-8246, Sandia National Laboratories, 1986.

[23] V. Giovangigli, N. Darabiha, in: C.-M. Brauner, C. Schmidt-Lainé (Eds.), Mathematical Modeling in Combustion and Related Topics, Nijhoff, Dordrecht, 1988, pp. 491–503.

[24] B.A.V. Bennett, Z. Cheng, R.W. Pitz, M.D. Smooke, Combust. Theory Model. 12 (3) (2008) 497–527.

[25] P. Deuflhard, Numerische Mathematik 22 (4) (1974) 289–315.

[26] M.D. Smooke, J. Optim. Theory Appl. 39 (4) (1983) 489–511.

[27] H.A. van der Vorst, SIAM J. Sci. Stat. Comput. 13 (2) (1992) 631–644.

[28] P.B. Kuhn, B. Ma, B.C. Connelly, M.D. Smooke, M.B. Long, Proc. Combust. Inst. 33 (2011) 743–750.

[29] B. Ma, G. Wang, G. Magnotti, R.S. Barlow, M.B. Long, Combust. Flame, 161 (4) (2014) 908–916.

Product references are for clarity and do not indicate an endorsement on the part of NASA or the federal government.